NJC

Accepted Manuscript

This is an *Accepted Manuscript*, which has been through the Royal Society of Chemistry peer review process and has been accepted for publication.

Accepted Manuscripts are published online shortly after acceptance, before technical editing, formatting and proof reading. Using this free service, authors can make their results available to the community, in citable form, before we publish the edited article. We will replace this *Accepted Manuscript* with the edited and formatted *Advance Article* as soon as it is available.

You can find more information about *Accepted Manuscripts* in the **Information for Authors**.

Please note that technical editing may introduce minor changes to the text and/or graphics, which may alter content. The journal's standard **Terms & Conditions** and the **Ethical guidelines** still apply. In no event shall the Royal Society of Chemistry be held responsible for any errors or omissions in this *Accepted Manuscript* or any consequences arising from the use of any information it contains.

Synthesis, structures, luminescent and molecular recognition properties of three new alkaline earth metal carboxyphosphonates with a 3D supramolecular structure

Hui Luo, Chao Ma, Cheng–Qi Jiao, Zhen–Gang Sun,* Tong Sun, Ming–Xue Ma, Yan–Yu Zhu, Wen–Zhu Li, Mei–Ling Wang, and Xiao–Wen Zhang

School of Chemistry and Chemical Engineering, Liaoning Normal University, Dalian 116029, P. R. China

Three new alkaline earth metal carboxyphosphonates with a 3D supramolecular structure, namely, $Ca[(H_3L)(H_2O)]$ **(1)**, $Sr[(H_3L)(H_2O)_2]$ **(2)** and $Ba[(H_3L)(H_2O)]$ **(3)** (H_5L= 4–{[bis(phosphonomethyl)amino]methyl}benzoic acid) have been synthesized under hydrothermal conditions. For compound **1**, $\{CaO_6\}$ and $\{CPO_3\}$ polyhedra are interconnected into a 1D double-chain *via* corner-sharing. Adjacent chains are further cross-linked *via* the organic backbone $\{-C_6H_4CH_2N(CH_2)_2-\}$ of the carboxyphosphonate ligands, generating a 2D layer. These neighboring 2D metal phosphonate layers are connected through hydrogen bonding interactions to form a 3D supramolecular structure. In compound **2**, two edge-sharing $\{SrO_7\}$ polyhedra form centrosymmetric $\{Sr_2O_{12}\}$ units. Then these $\{Sr_2O_{12}\}$ units are connected by phosphonate groups to form a 1D chain, which is further cross-linked through N atoms from carboxyphosphonate ligands to form a 2D inorganic layer. These 2D inorganic layers interdigitate through hydrogen bonding interactions to generate a 3D supramolecular structure. In compound **3**, the connections of $\{BaO_{10}\}$ and $\{CPO_3\}$ polyhedra form a 2D layer *via* corner-sharing and edge-sharing. Then adjacent layers are further assembled into a 3D supramolecular structure through hydrogen bonding interactions. The thermal stabilities and luminescence properties of compounds **1**–**3** were investigated. Interestingly, compounds **1**–**3** are selective and reversible for sensing of 1-butanol, 1-propanol and ethanol, respectively.

Introduction

The research of metal phosphonate hybrid compounds has emerged as a rapidly growing field of inorganic and materials chemistry, mainly due to their structure diversities and potential applications in catalysis, ion exchange, magnetism, proton conductivity, photochemistry and materials chemistry.[1]

---

* To whom correspondence should be addressed: E–mail: szg188@163.com

In the recent past, great efforts have been devoted to the syntheses of novel hybrid materials based on metal phosphonates. Therefore, the rational design and synthesis of novel metal phosphonates with the intriguing diversity of architectures and properties has become a particularly important subject. The nature of the organic ligands and the coordination trends of metal centers can affect the assembly of metal phosphonates to a considerable extent. In order to achieve this aim, the strategy of attaching functional groups such as amine, hydroxyl, crown ether, and carboxylate to the phosphonic acid has been found to be an effective method, since it can provide various kinds of coordination modes under different reaction conditions which may result in novel structures and interesting properties.[2] During the past few years, a series of metal phosphonates with functionalized phosphonic acids have been isolated in our laboratory.[3] Results from ours and other groups indicate that the carboxyphosphonic acids with additional carboxylic functional groups, such as $HOOC–R–PO_3H_2$, $HOOC–RN–(CH_2PO_3H_2)_2$ or $HOOC–RNHCH_2PO_3H_2$ (R = alkyl or aryl group), have been proved to be very useful ligands for the synthesis of metal phosphonates with framework structures.[4] Additionally, despite the selection and design of the promising phosphonate ligands, the choice of metal centers as nodes can also play a significant role in the assembly of metal phosphonates.[5] In previous literature, transition-metal ions attract wide attention in the researches of coordination polymers, due to the well-defined coordination geometries. While alkaline-earth (AE) metal ions are often ignored mainly for the following reasons. AE metal ions have larger radii which make it harder to predict their coordination numbers and geometries. Moreover, AE metal ions show high affinity for oxygen donors, especially water ligands, which is adverse to metal–ligand cross-linking for the extension of high-dimensional structures.[6] However, the unique coordination properties of AE atoms mentioned above attracted our interest greatly. AE metal ions, in particular Ca^{2+} and Sr^{2+}, also play an important role in bone mineral formation and Ca^{2+} metabolism.[7] Therefore, the study of AE metals phosphonates presents a fruitful area of research that has repercussions in several front-line disciplines. In this context, the role played by some noncovalent intermolecular forces is also very important, as the hydrogen bonding interactions increase the dimensionality of the polymerization. In the present paper, by employing $4–HO_2C–C_6H_4–CH_2N(CH_2PO_3H_2)_2$ (H_5L) as the phosphonate ligand, we have successfully obtained three new alkaline earth metal carboxyphosphonates with a 3D supramolecular structure, namely, $Ca[(H_3L)(H_2O)]$ **(1)**, $Sr[(H_3L)(H_2O)_2]$ **(2)** and $Ba[(H_3L)(H_2O)]$ **(3)**. Herein we report their syntheses, crystal structures, luminescent and molecular recognition properties. To date, only a few

investigations on molecular recognition properties of transition metal phosphonates have recently been reported by our group.[8] To the best of our knowledge, no alkaline earth metal phosphonate hybrids have been realized so far for their molecular recognition properties, and this is the first example of the studies on molecular recognition property of AE metal phosphonates.

Results and discussion

Syntheses

By using the $4-HOOCC_6H_4CH_2N(CH_2PO_3H_2)_2$ (H_5L) as the phosphonate ligand, three new alkaline earth metal carboxyphosphonates with a 3D supramolecular structure have been successfully synthesized under hydrothermal conditions. With the aim to explore an optimum method for obtaining pure phase materials, two systematical experimental investigations have been designed. The first experiment was designed to investigate the influence of the pH value on the reaction products. Thus, the system using $CaCl_2$ as calcium(II) salts keeping a constant Ca(II)/4,4'-bipy/H_5L = 1:0.5:0.5 ratio at different pH was studied (T=140 °C, 96 h). Unexpectedly, the pure phase of large block single crystals for compound **1** is obtained when pH was adjusted to 5.5 using 1M NaOH solution. However, the formation of amorphous powders or mixture phases for compound **1** comes into being at other pH values. So we realize that pH = 5.5 may be more adaptable pH value to synthesize compound **1**. One other variable that has a profound impact on the formation of suitable single–crystals for X–ray diffraction is the temperature. Compound **1** was obtained as a good sample for X–ray diffraction studies at the used reaction temperature of 140 °C. The results of two experimental investigations show that the pH = 5.5 is regarded as the optimal pH value to synthesize compound **1** keeping a constant Ca(II)/4,4'-bipy/H_5L = 1:0.5:0.5 ratio (T=140 °C, 96 h). The analogous experimental investigations were also designed to obtain the optimum method for synthesizing compounds **2** and **3**. Interestingly, 4,4'-bipy and piperazine also play a key role in the formation of compounds **1** and **2**, respectively. We tried to obtain them without the presence of 4,4'-bipy and piperazine, but no good samples for X–ray diffraction study were obtained. Even if the piperazine and 4,4'-bipy were not included in the final products, their inclusion in the reactive mixture is crucial to isolate good-quality single crystals of compounds **1** and **2**. In addition, despite our efforts to grow single–crystals of Mg^{2+} carboxyphosphonates under the similar hydrothermal conditions, we were not successful in obtaining good samples for X–ray diffraction studies. The

3

powder X–ray diffraction patterns (XRD) of compounds **1**–**3** all match those simulated from single–crystal X–ray data (Fig. S1–S3, ESI). The diffraction peaks on the patterns correspond well in position, confirming that the three title compounds are all pure phase.

Table 1 Crystal data and structure refinement for compounds **1**–**3**

Compounds	**1**	**2**	**3**
Chemical formula	$C_{10}H_{15}NO_9P_2Ca$	$C_{10}H_{17}NO_{10}P_2Sr$	$C_{10}H_{15}NO_9P_2Ba$
Formula weight	395.25	460.81	492.51
Crystal system	Triclinic	Triclinic	Triclinic
Space group	$P–1$	$P–1$	$P–1$
a / Å	6.9927(4)	6.0359(6)	5.4566(7)
b / Å	8.0857(5)	8.0803(8)	8.6781(12)
c / Å	14.2010(9)	16.5511(15)	16.081(2)
α (°)	101.0160(10)	93.878(2)	92.800(2)
β (°)	95.0910(10)	95.2730(10)	92.173(2)
γ (°)	101.3240(10)	102.285(2)	105.253(2)
V / Å^3	766.12(8)	782.25(13)	732.78(17)
Z	2	2	2
D_c / g·cm^{-3}	1.713	1.956	2.232
μ / mm^{-1}	0.665	3.705	2.977
$F(000)$	408	464	480
Refl. measured	4392	4472	4144
Unique refl. (R_{int})	3114(0.0140)	3190(0.0214)	2968(0.0200)
GOF on F^2	1.038	1.015	1.028
R_1, Rw [I>2σ (I)]	0.0325, 0.0847	0.0379, 0.0874	0.0529, 0.1508
R_1, Rw (all data)	0.0378, 0.0889	0.0503, 0.0929	0.595, 0.1557
($\Delta\rho$) max, min / e Å^{-3}	0.578, –0.861	0.756, –0.786	4.886, –1.349

$R_1 = \Sigma\ (|F_0|–|F_C|)\ /\ \Sigma\ |F_0|$; $wR_2 = [\Sigma\ w\ (|F_0|–|F_C|)^2\ /\ \Sigma\ w\ F_0^2]^{1/2}$.

Table 2 Hydrogen bond distances (Å) and angles (°) of compounds **1**–**3**

Compound **1**				
D–H···A	D(D–H)/ Å	d(H···A)/ Å	D–H···A/ °	d(D···A)/ Å
O(9)–H(9A)···O(3)#5	0.85	2.098	162.59	2.920
O(9)–H(9B)···O(5)#6	0.85	2.222	120.96	2.758
Compound **2**	D(D–H)/ Å	d(H···A)/ Å	D–H···A/ °	d(D···A)/ Å
O(8)–H(8)···O(1)#7	0.82	1.770	168.50	2.581(4)
Compound **3**	D(D–H)/ Å	d(H···A)/ Å	D–H···A/ °	d(D···A)/ Å
O6–H6A···O(8)#9	0.85	1.875	146.89	2.628

Description of the crystal structures

Description of structure 1

X–ray single crystal diffraction revealed that compound **1** crystallizes in the triclinic space group P–1 (see Table 1). As shown in Fig. 1, the asymmetric unit of compound **1** contains one crystallographically independent Ca(II) cation, one H_3L^{2-} anion and one coordinated water molecule. The Ca(II) cation exhibits six–coordinated environment. Five of the six coordination positions are filled with four phosphonate oxygen atoms (O2, O5, O3A and O6B) and one carboxylate oxygen atom (O7C) from four separate H_3L^{2-} anions, and the remaining site is occupied by O9 atom from the coordinated water molecule. The Ca–O bond distances fall between 2.2838(15) and 2.4109(17) Å (Table S1, ESI). These values are in agreement with those reported for other Ca(II) phosphonates.[9] The H_3L^{2-} acts as a pentadentate bridging mode and links with four Ca(II) cations through four phosphonate oxygen atoms (O2, O3, O5 and O6) and one carboxylate oxygen atom (O7). The oxygen atoms (O2, O3, O5, O6 and O7) are all monodentate (Fig. 2a). The phosphonate oxygen atoms (O1 and O4) and nitrogen atom (N1) are protonated based on P–O distances and charge balance.
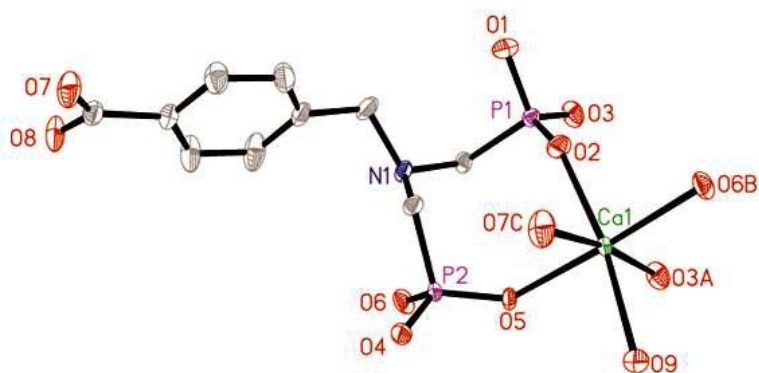
Fig. 1 Structure unit of compound **1** showing the atom labeling. Thermal ellipsoids are shown at the 50% probability level. All H atoms are omitted for clarity. Symmetry code for the generated atoms: (A) –x + 2, –y + 1, –z + 1; (B) x – 1, y, z; (C) –x + 1, –y + 1, –z.
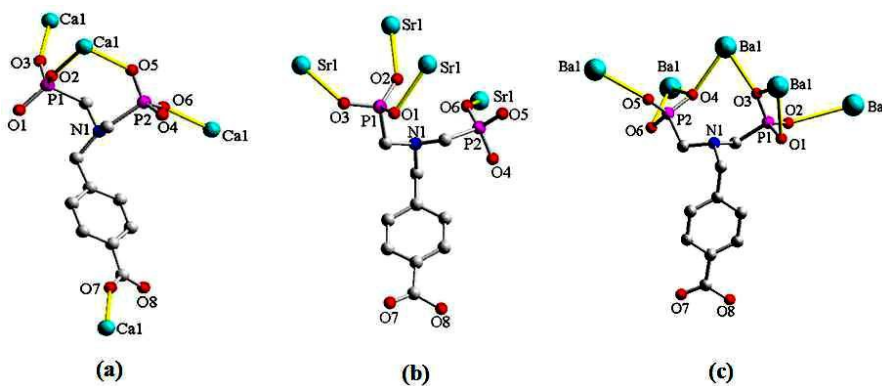
Fig. 2 The coordination modes of H_5L ligands in compound **1** (a), compound **2** (b), and compound **3** (c).
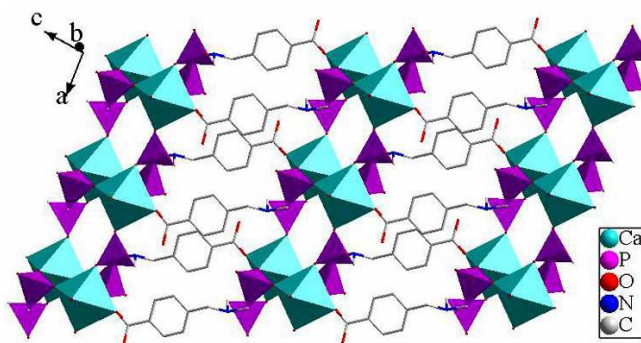
Fig. 3 (a) View of the 2D layer structure for compound **1** in the a*c*-plane.
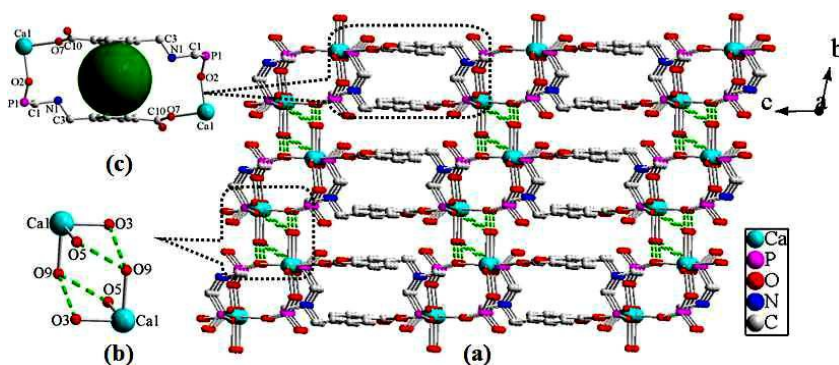
Fig. 4 (a) View of the 3D supramolecular structure for compound **1** along the *a*-axis *via* the interactions of hydrogen bonds; (b) The connectivity of hydrogen bonds for compound **1**; (c) The 24-atom rings in compound **1**.

Compound **1** exhibits a 3D supramolecular structure. {CaO_6} octahedra and {CPO_3} tetrahedra are interconnected into a 1D double-chain along the *a*-axis *via* corner-sharing. Adjacent so-built chains are further cross-linked *via* the organic backbone {$-C_6H_4CH_2N(CH_2)_2-$} of the carboxyphosphonate ligands, generating a 2D layer (Fig. 3). Such neighboring 2D metal phosphonate layers are connected through hydrogen bonding interactions to give rise to a 3D supramolecular structure (Fig. 4a). As shown in Fig. 4b, there are hydrogen bonds between the oxygen atoms (O9) of coordinated water molecules and the phosphonate oxygen atoms (O3 and O5) from the carboxyphosphonate ligands with the distances of 2.920 Å (O9–H9A···O3), 2.758 Å (O9–H9B···O5) and corresponding angles of 162.59° and 120.96° (Table 2), respectively. Compound **1** also contains a 1D channel system along the *a*-axis (Fig. 4c), which is formed by 24-membered rings composed of two Ca(II) cations and two {$OOCC_6H_4CH_2NCPO_3$} units from two H_3L^{2-} ligands. The size of the channel is estimated to be 11.3 Å (O2–O2) × 6.2 Å (C3−C10) based on structure data.

Description of structure 2

Compound **2** crystallizes in the triclinic space group *P*−1 (see Table 1). As shown in Fig. 5, the asymmetric unit of the structure for compound **2** contains one Sr(II) cation, one H_3L^{2-} anion and two coordinated water molecules. Sr(II) cation is seven–coordinated by four phosphonate oxygen atoms (O1, O2A, O3B and O6C) from four separate H_3L^{2-} anions and three oxygen atoms (O9, O9A and O10) from three coordinated water molecules. The Sr–O distances are in the range of

7

2.550(3) to 2.629(3) Å (Table S2, ESI). These distances are comparable to those reported for other Sr(II) phosphonates.[10] The H_3L^{2-} serves as a tetradentate ligand, bridging with four Sr(II) cations through four phosphonate oxygen atoms (O1, O2, O3 and O6). The phosphonate oxygen atoms (O1, O2, O3 and O6) are all monodentate (Fig. 2b). The carboxylate oxygen atoms (O7, O8) are not involved in the coordination of the metal cations. The phosphonate oxygen atoms (O4 and O5) and the carboxylate oxygen atom (O8) are protonated based on the requirement of charge balance.
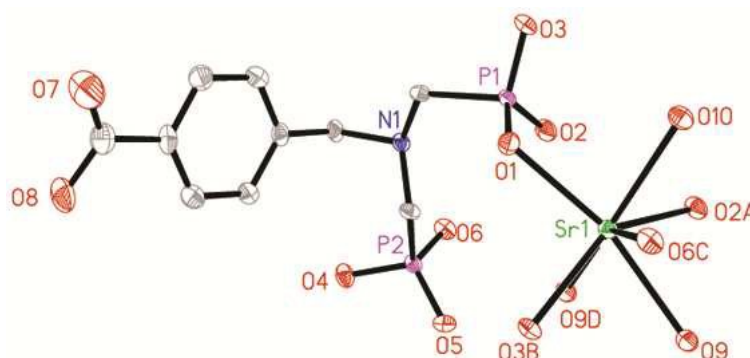
Fig. 5 Structure unit of compound **2** showing the atom labeling. Thermal ellipsoids are shown at the 50% probability level. All H atoms are omitted for clarity. Symmetry code for the generated atoms: (A) –x, –y + 1, –z + 1; (B) x + 1, y, z; (C) x, y – 1, z; (D) –x + 1, –y + 1, –z + 1.
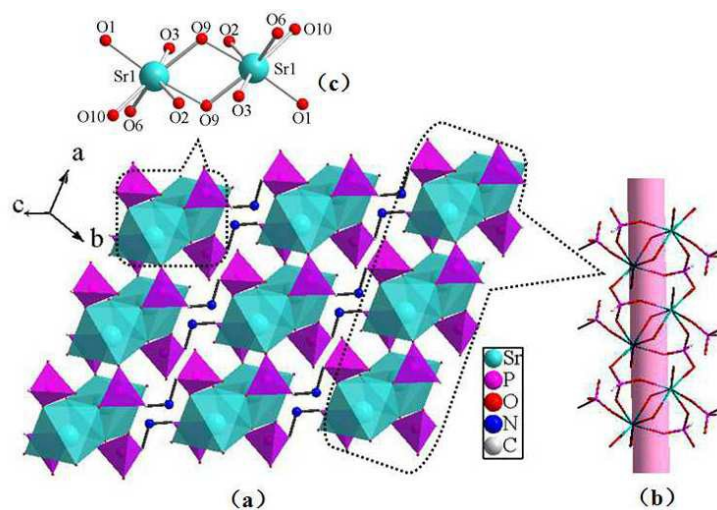
Fig. 6 (a) View of the 2D layer structure of compound **2** in the *ab*-plane; (b) The 1D chain structure of compound **2** along the *a*-axis.

The overall structure of compound **2** can be described as a 3D supramolecular structure. Two edge-sharing $\{SrO_7\}$ polyhedra form centrosymmetric $\{Sr_2O_{12}\}$ units (Fig. 6a), the oxygen O9 acts as a μ_2 ligand bridging two Sr(II) cations of the $\{Sr_2O_{12}\}$ units. Then $\{Sr_2O_{12}\}$ units are connected by phosphonate groups to form a 1D chain along the *a*-axis (Fig. 6b), which are further cross-linked through N atoms from carboxyphosphonate ligands to form a 2D inorganic layer in the *ab*-plane (Fig. 6c). The organic units point into the interlayer space with the carboxylic acid groups directed to the adjacent layers. The neighboring 2D inorganic layers interdigitate through hydrogen bonding interactions to give rise to a 3D supramolecular structure (Fig. 7a). As shown in Fig. 7b, there are hydrogen bonds between the carboxylate oxygen atoms (O8) and the phosphonate oxygen atoms (O1) from the carboxyphosphonate ligands with the distances of 2.581 Å (O8–H8⋯O1) and corresponding angles of 168.50° (Table 2).
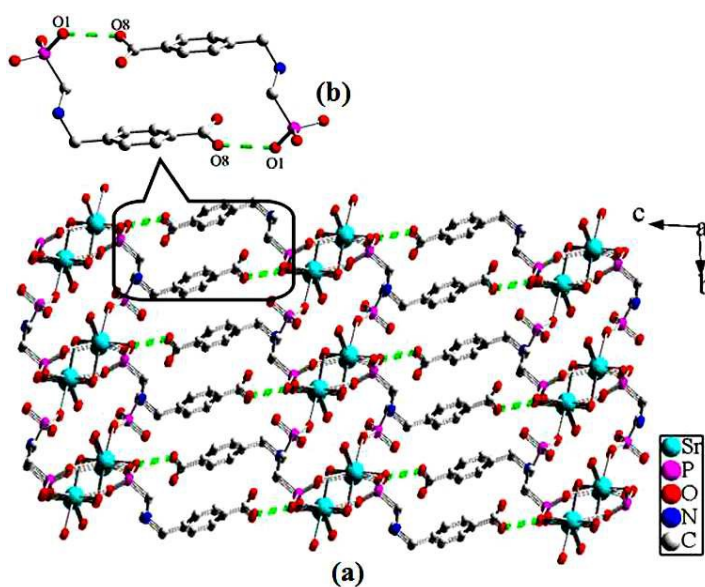
Fig. 7 (a) View of the 3D supramolecular structure for compound **2** along the *a*-axis *via* the interactions of hydrogen bonds; (b) The connectivity of hydrogen bonds for compound **2**.

Description of structure 3

Compound **3** crystallizes in the triclinic space group *P*−1 (see Table 1). As shown in Fig. 8, the asymmetric unit of the structure for compound **3** is comprised of one Ba(II) cation, one H_3L^{2-} anions and one coordinated water molecules. The Ba(1) cation is ten–coordinated by eight phosphonate oxygen atoms (O1A, O2B, O3A, O3C, O4, O4C, O5D, and O6) from five separate H_3L^{2-} anions. The remaining sites are occupied by two oxygen atoms (O9 and O9E) from two

coordinated water molecules. The Ba–O distances range from 2.733(6) to 3.110(6) Å (Table S3, ESI), which are comparable to those reported for other barium(II) phosphonates.[11] In compound **3**, the coordination mode of the H_3L^{2-} anion can be described as an octadentate bridging mode. It links five Ba(II) cations through all its phosphonate oxygen atoms (Fig. 2c). The two phosphonate oxygen atoms (O3, O4) of the phosphonate group behave as μ_2 metal linkers, whereas the remaining phosphonate oxygen atoms (O1, O2, O5 and O6) are unidentate. The phosphonate oxygen atoms (O1, O5) and the carboxylate oxygen atom (O8) are protonated based on the requirement of charge balance.
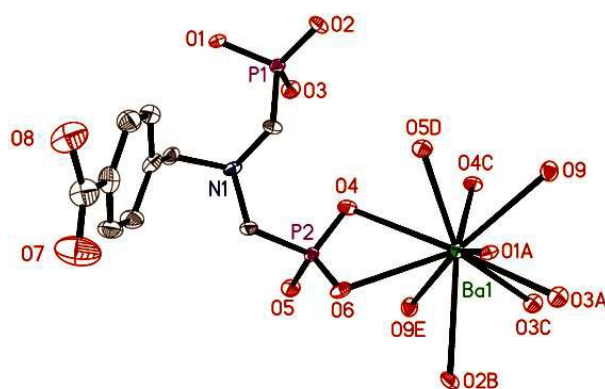
Fig. 8 Structure unit of compound **3** showing the atom labeling. Thermal ellipsoids are shown at the 50% probability level. All H atoms are omitted for clarity. Symmetry code for the generated atoms: (A) –x + 1, –y + 1, –z; (B) x –1, y, z; (C) x, y + 1, z; (D) x + 1, y, z; (E) x + 1, y + 1, z.
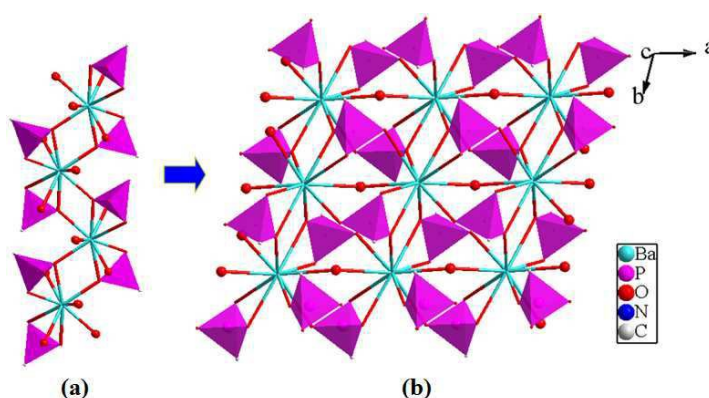
Fig. 9 (a) View of the 1D chain structure of compound **3** along the *b*-axis; (b) The 2D layer structure of compound

    3 in the *ab*-plane.

The compound **3** can be regarded as a 3D supramolecular network. The {BaO$_{10}$} and {CPO$_3$} polyhedra are interconnected into a 1D chain along the *b*-axis *via* corner-sharing (Fig. 9a). These chains are further linked into *via* edge-sharing to generate a 2D layer in the *ab*-plane (Fig. 9b). Then adjacent layers are further assembled into a 3D supramolecular structure through hydrogen bonding interactions (Fig. 10a). The carboxylate moieties of the H$_3$L^{2-} anions are orientated into the interlayer space. The organic units point into the interlayer space with the carboxylic acid groups directed to the adjacent layers. As shown in Fig. 10b, there are hydrogen bonds between the phosphonate oxygen atoms (O6) from the carboxyphosphonate ligands and the carboxylate oxygen atoms (O8) with the distances of 2.628 Å (O6–H6A⋯O8) and corresponding angles of 146.89° (Table 2).
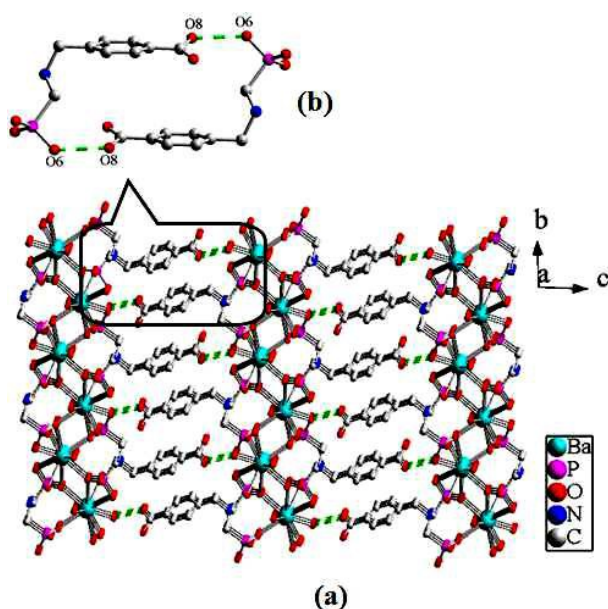
Fig. 10 (a) View of the 3D supramolecular structure for compound **3** along the *a*-axis *via* the interactions of hydrogen bonds; (b) The connectivity of hydrogen bonds for compound **3**.

Comparing with each other: with the larger radii, their (Ca^{2+} in **1**, Sr^{2+} in **2** and Ba^{2+} in **3**) coordination numbers are ranged from 6 to 10. Moreover, in their structures, AE metal ions are all coordinated to oxygen atoms from water ligands. While in some other similar transition-metals-based systems,[8a] it's easy to find that their coordination numbers are 6 or less than 6, and the affinity of transition-metals for oxygen donors, especially water ligands, are not as good as AE metal ions. Although compounds **1**–**3** are all 3D supramolecular framework, their structure are also different.

IR spectra

The IR spectra for compounds **1–3** are recorded in the region 4000–400 cm^{-1} (Fig. S4–S6, ESI). The absorption band at 3454 cm^{-1} for **1**, 3352 cm^{-1} for **2** and 3401 cm^{-1} for **3** can be assigned to the O–H stretching vibrations. The C–H stretching vibrations are observed as sharp, weak bands close to 3000 cm^{-1} for compounds **1–3**. The absorption bands at 1720 and 1435 cm^{-1} for the free carboxylate group in the free ligand,[12] have been shifted obviously to 1682 and 1425 cm^{-1} in compound **1**. Its rather low position is typical for constellations where the oxygen atoms of the carboxylate group coordinated to the metal.[13] Thus the carboxylate groups are deprotonated and in agreement with structural results for compound **1**. The absorption bands at 1717 cm^{-1} and 1438 cm^{-1} in compound **2**; and 1713 and 1415 cm^{-1} for compound **3**, which are the expectative value for the non-coordination of the carboxylate groups in compounds **2** and **3**.[14] The set of bands between 1200 and 900 cm^{-1} for three title compounds are due to stretching vibrations of the tetrahedral {CPO$_3$} groups, as expected.[15] Additional medium and weak bands at low energy for compounds **1–3** are found, which are likely assigned to bending vibrations of the tetrahedral {CPO$_3$} groups.

Thermal analysis

Thermogravimetric analysis diagram of compounds **1–3** have been performed in the temperature range of 50–1100 °C in static air atmosphere (Fig. S7–S9, ESI). The TG diagram of compound **1** exhibits one main continuous weight loss, which can be attributed to the loss of coordinated water, elimination of the organic moieties and the collapse of the structures. The weight loss started at about 236 °C and ended at 876 °C. The total weight loss of 56.4% is larger than the calculated value (49.9%) if the final products are assumed to be Ca(PO$_3$)$_2$. Compound **2** was thermally stable up to 163 °C. Above this temperature, the TG curve shows three steps of weight losses. At approximately 217 °C, it completes its first step of weight loss, corresponding to the release of two coordinated water molecules. The observed weight loss of 8.1% is basically close to the calculated value (7.8%). A second weight loss occurs between 296 and 730 °C, which can be attributed to the partial decomposition of the organic moieties and the collapse of the structures. The third stage occurring between 846 and 978 °C corresponds to the further decomposition of the compound. The total weight loss of 46.6% is almost consistent with the calculated value (46.7%) if the final products are assumed to be Sr(PO$_3$)$_2$. Compound **3** indicates two complicated overlapping steps of weight losses. The first step started at 181 °C and was completed at 262 °C, corresponding to the release of one

coordinated water molecules. The observed weight loss of 5.3% is basically consistent with the calculated value (3.7%). Above the temperature of 307 °C, a continuous weight loss was observed up to 880°C, corresponding to the decomposition of organic groups and the collapse of the structures. The total weight loss of 42.7% is close to the calculated value (40.1%) if the final products are assumed to be $Ba(PO_3)_2$. The thermal decomposition products of compounds **1**–**3** are amorphous and were not further characterized. In addition, to further understand the thermal stability of compounds **1**–**3**, powder X–ray diffraction (PXRD) studies were also performed (Fig. S10–S12, ESI). In compound **1**, from room temperature to 160 °C, no change occurs and the powder X–ray diffraction (PXRD) patterns for the calcined sample of compound **1** are in agreement with that of the as-synthesized sample. The patterns change when the temperature reaches 180 °C, which indicates that the structure of compound **1** was thermally stable up to 160 °C (Fig. S10, ESI). Then the PXRD patterns also demonstrate that there are retention of framework structure of compound **2** at 120 °C and compound **3** at 180 °C (Fig. S11 and Fig. S12, ESI).
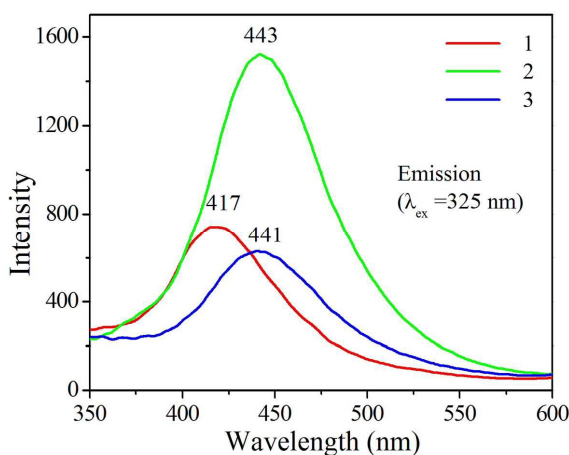
Fig. 11 Solid–state emission spectra of compounds **1**–**3** at room temperature.

Luminescent properties

Luminescent properties of coordination polymers have attracted much attention due to their potential optical applications.[16] It has been reported that the emission wavelength and intensity of the organic material can be affected through the coordination with metal. The solid-state luminescent properties of compounds **1**–**3** were investigated at room temperature (Fig. 11).

13

The free carboxyphosphonate ligand (H₅L) displays fluorescent emission bands at 337 and 349 nm upon excitation at 308 nm (Fig. S13, ESI), which may be attributed to ligand-centered $\pi^* \rightarrow n$ or $\pi \rightarrow \pi^*$ electronic transitions. In contrast, compounds **1–3** give broad fluorescent emissions under the same experimental conditions. As shown in Fig. 11, upon excitation at 325 nm, compounds **1–3** exhibit blue fluorescence emission bands at λ_{max} = 417 nm, λ_{max} = 441 nm and λ_{max} = 443 nm, respectively. It is clear that compounds **1–3** show a red-shifted emission band to different extents with slightly weakened intensities compared with the free carboxyphosphonate ligand, which probably originated from the ligand-to-metal charge transfer (LMCT).[17] Unfortunately, the luminescent lifetimes of compounds **1–3** are not observed, since the lifetimes of compounds **1–3** are too short to be measured. The emission spectra of the three title compounds show varying degrees of red shift in comparison with the carboxyphosphonate ligand, which may because that the coordination of carboxyphosphonate ligands to metal cations affect the energy levels of the ligands.[18] It is interesting to note that the emission intensities for compounds **1–3** present different changes with the free ligand. The differences in the structures of compounds **1–3** result in this phenomenon because the luminescence behavior is closely associated with the metal cations and the ligands coordinated. Furthermore, the difference in the relative intensities and positions of the peaks in the emission spectra of compounds **1–3** is probably due to the introduction of different metal centers and the structure of the complexes.[19] Although compounds **1–3** are all 3D supramolecular structures, their metal centers are Ca^{2+}, Sr^{2+} and Ba^{2+}, respectively. What's more, they contain different coordination numbers (6 for **1**, 7 for **2** and 10 for **3**), and their coordination environment are also different. Therefore, luminescence mechanisms of compounds **1–3** should be assigned the ligand-to-metal charge transfer (LMCT) and the luminescence behavior is closely associated with the metal cations and the ligands coordinated around them.

Molecular Recognition Properties

To examine the potential of compounds **1–3** for the sensing of alkyl alcohol, compounds **1–3** were immersed in different alkyl alcohol solvent for luminescence studies. Under the same measurement, the luminescent properties of methanol, ethanol, 1-propanol, 1-butanol, and 1-pentanol suspensions at room temperature are shown in Fig. 12a, 12b and 12c, respectively. The suspensions were prepared by introducing 1.0 mg of the sample (such as compound **1**) powder into 4.0 mL of methanol, ethanol, 1-propanol, 1-butanol, and 1-pentanol at room temperature, the

luminescent studies of compounds **1–3** in different alkyl alcohol suspensions were investigated (Fig. 12). The emission spectra of alcohol solvents are shown in Fig. S14 (ESI).

As shown in the Fig. 12 and Fig. S14 (ESI), the luminescent properties of suspensions are heavily dependent on the identity of the solvent molecule. Comparing the luminescent intensity of alkyl alcohol (Fig. S15, ESI) and compounds **1–3** in alkyl alcohol suspensions (Fig. 12a, 12b and 12c), which exhibit the most noticeable weakening or enhancing effects of compound **1** in 1-butanol, compound **2** in 1-propanol and compound **3** in ethanol suspensions. Such solvent-dependent luminescence properties are very fascinating and considerable for the selective sensing of 1-butanol, 1-propanol and ethanol solvent molecules. Then we examined the molecular recognition properties of compound **1** in 1-butanol, compound **2** in 1-propanol and compound **3** in ethanol solvent molecules in detail for further exploration. Compound **1** (1.0 mg) was dispersed in 2.5 mL, 3.0 mL, 3.5 mL and 4.0 mL 1-butanol solvent, while the 1-butanol solvent content was gradually increased to monitor the emissive response. As shown in Fig. 13a, the luminescent intensity of compound **1** in 1-butanol suspensions gradually increased with the addition of 1-butanol solvent. While the content of 1-propanol solvent in the suspensions of compound **2** was increased, the luminescent intensity was evidently weakened (Fig. 13b). Then when we improved the content of ethanol solvent in the suspensions of compound **3**, the luminescent intensity was gradually weakened (Fig. 13c).

Although the mechanism for such weakening and enhancing effects of alkyl alcohol molecules is still not clear at this moment, but this phenomenon may be due to the differences in structures of compounds **1–3**. The overall structures of compounds **1–3** are all 3D supramolecular structures, but they contain different numbers of coordinated water molecules and there are uncoordinated –COOH groups of compounds **2** and **3**. The existence of hydrogen bonding between compounds and the guest molecules may enhance the interaction. The luminescence weakening for 1-butanol or enhancing for 1-propanol and ethanol could be ascribed to the energy transfer though O–H···O hydrogen bonding interactions among coordinated water molecules, –COOH groups and alkyl alcohol solvent molecules, as in the case of ionic sensing through hydrogen bonding interactions.[19] Other solvents (such as methanol) may also be incorporated in the framework by hydrogen bonding interactions, but the effects are not significant as compared to 1-butanol in compound **1**, 1-propanol in compound **2**, and ethanol in compound **3**. Although the detailed mechanism for such effect of small solvent molecules is in depth study, the binding interaction of the complexes with guest solvent molecules definitely plays an vital role.[21] To check the structural transformation, PXRD

measurements of compound **1**–**3** in 1-butanol, 1-propanol and ethanol after aging were also done, respectively. Powder X–ray diffraction shows obviously weakened intensity than the original one, which is due to the interaction of compounds with the solvent molecule (Fig. S16–S18, ESI).[8c] Therefore, compounds **1**–**3** can be good materials to be used for the sensing of 1-butanol, 1-propanol and ethanol, respectively. The highly sensing function of compounds **1**–**3** indicates the promise of this type of luminescent materials for the sensing of substrates in biological systems.[22]

It is worth mentioning that the Power XRD patterns of compounds obtained after the introduction of various solvents are almost identical to that of as-synthesized **1**–**3** (Fig. S19–S21, ESI), indicating that the original framework remains unchanged upon solvent treatment.[20a, 23]
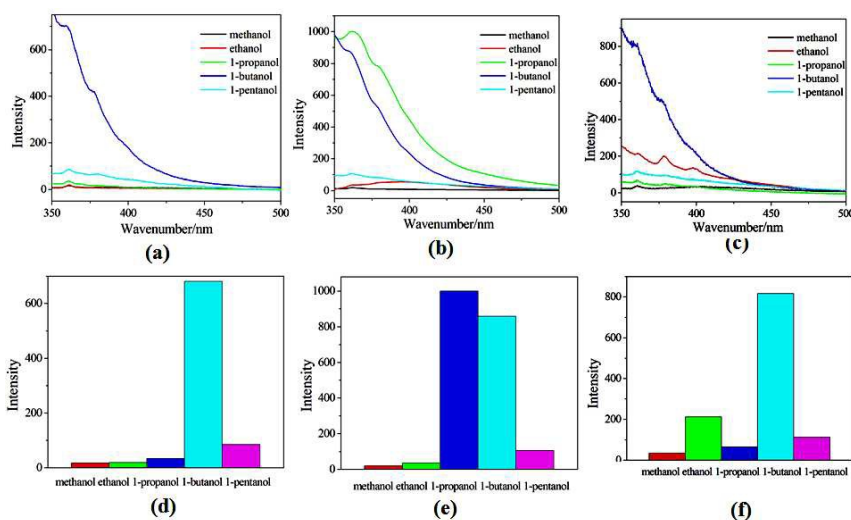
Fig. 12 The emission spectra of (a) compound **1** suspensions, (b) compound **2** suspensions and (c) compound **3** suspensions. The transition intensities of (d) compound **1**, (e) compound **2**, and (f) compound **3** introduced into various pure alcohol solvents when excited at 325 nm.
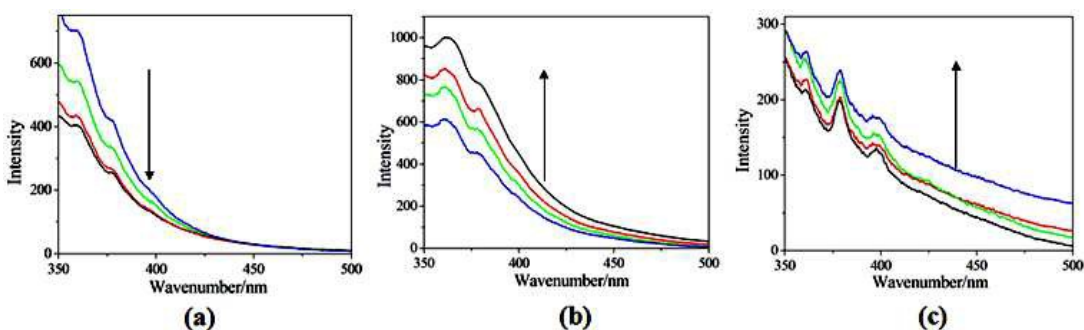
Fig. 13 The fluorescence properties of (a) compound **1** suspensions in the presence of various amounts of 1-butanol, (b) compound **2** suspensions in the presence of various amounts of 1-propanol, (c) compound **3** suspensions in the presence of various amounts of ethanol solvent (increasing in steps of 0.5 mL from 2.5 to 4.0 mL).

Conclusion

In summary, three new alkaline earth metal carboxyphosphonates with a 3D supramolecular structure, namely, $Ca[(H_3L)(H_2O)]$ (**1**), $Sr[(H_3L)(H_2O)_2]$ (**2**) and $Ba[(H_3L)(H_2O)]$ (**3**) have been synthesized *via* hydrothermal technique using $4–HO_2C–C_6H_4–CH_2N(CH_2PO_3H_2)_2$ as the phosphonate ligand. For compound **1**, $\{CaO_6\}$ and $\{CPO_3\}$ polyhedra are interconnected into a 1D double-chain. Adjacent so-built chains are further cross-linked *via* the organic backbone $\{-C_6H_4CH_2N(CH_2)_2-\}$ of the carboxyphosphonate ligands, generating a 2D layer. Then the adjacent 2D metal phosphonate layers are connected through hydrogen bonding interactions to form a 3D supramolecular structure. In compound **2**, two edge-sharing $\{SrO_7\}$ polyhedra form centrosymmetric $\{Sr_2O_{12}\}$ units. Then these $\{Sr_2O_{12}\}$ units are connected by phosphonate groups to form a 1D chain, which is further cross-linked through N atoms from carboxyphosphonate ligands to form a 2D inorganic layer. These 2D inorganic layers interdigitate through hydrogen bonding interactions to generate a 3D supramolecular structure. Compound **3** also shows a 3D supramolecular structure. The connections of $\{BaO_{10}\}$ and $\{CPO_3\}$ polyhedra form a 2D layer *via* corner-sharing and edge-sharing. These neighboring layers are further assembled into a 3D supramolecular structure through hydrogen bonding interactions. The luminescence properties indicate that they exhibit blue fluorescence emission bands, and their luminescence mechanisms should be assigned the ligand-to-metal charge transfer (LMCT). Furthermore, compounds **1–3** can be potential materials to be used for the sensing of 1-butanol, 1-propanol and ethanol, respectively.

Experimental

Materials and measurements

The 4–{[bis(phosphonomethyl)amino]methyl}benzoic acid) (H_5L) was synthesized according to a published method.[24] All other chemicals were obtained from commercial sources and used without further purification. C, H and N content were determined by using a PE–2400 elemental analyzer. Ca, Sr, Ba and P content were determined by using an inductively coupled plasma (ICP) atomic absorption spectrometer. IR spectra were recorded on a Bruker AXS TENSOR–27 FT–IR spectrometer with KBr pellets in the range 4000–400 cm^{-1}. The X-ray powder diffraction data was collected on a Bruker AXS D8 Advance diffractometer using Cu–Kα radiation ($\lambda = 1.5418$ Å) in the 2θ range of 5–60° with a step size of 0.02° and a scanning rate of 3°/min. TG analyses were

performed on a Perkin–Elmer Pyris Diamond TG–DTA thermal analyses system in static air with a heating rate of 10 K min^{-1} from 50 °C to 1100 °C. The luminescence analyses were performed on a HITACHI F–7000 spectrofluorometer. The luminescent properties of compounds **1–3** in solvent suspensions were investigated at room temperature. The suspensions were prepared by introducing the sample (1.0 mg) as a powder into different solvents (each 4.0 mL). The fluorescence spectra of the suspensions were measured after aging overnight.

Synthesis

Ca[(H$_3$L)(H$_2$O)] (1). A mixture of CaCl$_2$ (0.11 g, 1 mmol), H$_5$L (0.17 g, 0.5 mmol) and 4,4'-bipy (0.09 g, 0.5 mmol) in 10 mL of distilled water, adjusted to a pH of 5.5 using NaOH solution, was stirred for about 1 hour at room temperature, sealed in a 20 mL Teflon–lined stainless steel autoclave and heated at 140 °C for 4 days under autogenous pressure. After the mixture was cooled slowly to room temperature, the colorless block crystals of **1** were obtained. Yield 55.6 % (based on Ca). Anal. Calc. for C$_{10}$H$_{15}$N$_2$O$_9$P$_2$Ca: C, 30.39; H, 3.83; N, 3.54; P, 15.67; Ca, 10.14. Found: C, 30.35; H, 3.86; N, 3.58; P, 15.63; Ca, 10.18 %. IR (KBr, cm^{-1}): 3454(m), 3234(m), 3111(m), 3062(w), 2940(w), 2989(w), 1682(s), 1609(m), 1572(m), 1425(m), 1377(s), 1255(s), 1157(s), 1093(s), 1042(s), 925(s), 815(m), 766(s), 705(s), 595(m), 546(s), 498(s).

Sr[(H$_3$L)(H$_2$O)$_2$] (2). A mixture of SrCl$_2$·6H$_2$O (0.27 g, 1 mmol), H$_5$L (0.17 g, 0.5 mmol) and piperazine (0.08 g, 1 mmol) was dissolved in 10 mL distilled water , and then stirred for about 1 hour at room temperature. The mixture (pH = 5.0) was sealed in a 20 mL Teflon–lined stainless steel autoclave, and heated at 140 °C for 4 days under autogenous pressure. After the mixture was cooled slowly to room temperature, the colorless block crystals of **2** were obtained. Yield 58.9% (based on Sr). Anal. Calc. for C$_{10}$H$_{17}$NO$_{10}$P$_2$Sr: C, 26.06; H, 3.72; N, 3.04; P, 13.44; Sr, 19.01. Found: C, 26.02; H, 3.75; N, 3.06; P, 13.40; Sr, 19.06 %. IR (KBr, cm^{-1}): 3352(m), 3221(m), 3026(w), 2968(w), 2920(w), 2795(w), 1717(s), 1658(m), 1569(w), 1462(m), 1438(m), 1376(m), 1297(m), 1181(s), 1108(s), 986(s), 803(s), 680(m), 620(s), 533(m), 501(m), 460(m).

Ba[(H$_3$L)(H$_2$O)] (3). A mixture of BaCl$_2$·2H$_2$O (0.25 g, 1 mmol) and H$_5$L (0.17 g, 0.5 mmol) was dissolved in 10 mL distilled water, and then stirred for about 1 hour at room temperature. The mixture (pH = 2.5) was sealed in a 20 mL Teflon–lined stainless steel autoclave, and heated at 140 ℃ for 4 days under autogenous pressure. After the mixture was cooled slowly to room temperature, the colorless needle crystals of **3** were obtained. Yield 35.1% (based on Ba). Anal. Calc. for

$C_{10}H_{15}NO_9P_2Ba$: C, 24.39; H, 3.07; N, 2.84; P, 12.58; Ba, 27.88. Found: C, 24.35; H, 3.03; N, 2.89; P, 12.63; Ba, 27.83 %. IR (KBr, cm^{-1}): 3401(m), 3026(m), 2978(m), 2941(w), 2858(m), 1713(s), 1621(w), 1514(w), 1415(m), 1279(s), 1157(s), 1084(s), 974(w), 867(m), 803(m), 730(s), 570(s), 522(m), 449(m).

X-Ray crystallography

Data collections for compounds **1**–**3** were performed on the Bruker AXS Smart APEX II CCD X–diffractometer equipped with graphite monochromated Mo*Kα* radiation (λ = 0.71073 Å) at 293 ± 2K. An empirical absorption correction was applied by using the SADABS program. All structures were solved by direct methods and refined by full–matrix least squares fitting on F^2 by SHELXS–97.[25] All non–hydrogen atoms were refined anisotropically. Hydrogen atoms of organic ligands were generated geometrically with fixed isotropic thermal parameters, and included in the structure factor calculations. Hydrogen atoms for water molecules were not included in the refinement. CCDC 1043122–1043124 contain the supplementary crystallographic data for this paper. These data can be obtained free of charge www.ccdc.cam.ac.uk/conts/retrieving.html (or from the Cambridge Crystallographic Data Center, 12, Union Road, Cambridge CB21EZ, UK; fax: (+44) 1223-336-033; e-mail: deposit@ccdc.cam.ac.uk).

References

1. (a) M. Bazaga-García, R. M. P. Colodrero, K. D. Demadis, *J. Am. Chem. Soc.*, 2014, **136**, 5731; (b) K. H. Zangana, E. M. Pineda and R. P. Winpenny, *Dalton Trans.*, 2014, **43**, 17101; (c) A. Clearfield and K. Demadis, *Metal Phosphonate Chemistry: From Synthesis to Applications*, Royal Society of Chemistry, Oxford, 2012, p. 164; (d) J. T. Rhule, C. L. Hill, D. A. Judd, *Chem. Rev.,* 1998, **98**, 327; (e) H. Hirao and K. Morokuma, *J. Am. Chem. Soc.,* 2010, **132**, 17901; (f) P. O. Adelani and T. E. Albrecht-Schmitt, *Inorg. Chem.,* 2010, **49**, 5701.

2. (a) F. Niekiel and N. Stock, *Cryst. Growth Des.*, 2014, **14**, 599; (b) J. Weber, G. Grossmann, K.

D. Demadis, N. Daskalakis, E. Brendler, M. Mangstl and J. S. Aufder. Günne, *Inorg. Chem.,* 2012, **51**, 11466; (c) P. O. Adelani and T. E. Albrecht-Schmitt, *Cryst. Growth Des.,* 2011, **11**, 4676; (d) S. F. Tang, X. B. Pan, X. X. Lv, S. H. Yan, X. R. Xu, L. J. Li and X. B. Zhao, *CrystEngComm.*, 2013, **15**, 1860.

3.　(a) W. Chu, Z. G. Sun, C. Q. Jiao, Y. Y. Zhu, S. H. Sun, H. Tian and M. J. Zheng, *Dalton Trans.*, 2013, **42**, 8009; (b) M. J. Zheng, Y. Y. Zhu, Z. G. Sun, J. Zhu, C. Q. Jiao, W. Chu, S. H. Sun and H. Tian, *CrystEngComm.*, 2013, **15**, 1445; (c) F. Tong, Z. G. Sun, K. Chen, Y. Y. Zhu, W. N. Wang, C. Q. Jiao, C. L. Wang and C. Li, *Dalton Trans.,* 2011, **40**, 5059; (d) K. Chen, Z. G. Sun, Y. Y. Zhu, Z. M. Liu, F. Tong, D. P. Dong, J. Li, C. Q. Jiao, C. Li and C. L. Wang, *Cryst. Growth. Des.,* 2011, **11**, 4623.

4.　(a) P. O. Adelani, A. G. Oliver, T. E. Albrecht-Schmitt, *Cryst. Growth Des.,* 2011, **11**, 1966; (b) H. Tan, W. Chen, D. Liu, Y. Li, E. Wang, *Datlon Trans.,* 2010, **39**, 1245; (c) N. G. Armatas, D. G. Allis, A. Prosvirin, G. Carnutu, C. J. O'Connor, K. Dunbar, J. Zubieta, *Inorg. Chem.,* 2008, **47**, 832.

5.　(a) S. F. Tang, J. J. Cai, L. J. Li, X. X. Lv, C. Wang and X. B. Zhao, *Dalton Trans.*, 2014, **43**, 5970; (b) T. Zheng, S. S. Bao, M. Ren and L. M. Zheng, *Dalton Trans.*, 2013, **42**, 16396; (c) Y. F. Liu, P. F. Yan and J. S. Gao, *Cryst. Growth Des.*, 2013, **13**, 3816.

6.　(a) N. S. Poonia and A. V. Bajaj, *Chem. Rev.*, 1979, **79**, 389; (b) X. Zhang, Y. Y. Huang, M. J. Zhang, J. Zhang and Y. G. Yao, *Cryst. Growth Des.*, 2012, **12**, 3231; (c) K. D. Demadis, S. D. Katarachia, R. G. Raptis, H. Zhao, and P. Baran, *Cryst. Growth Des.*, 2006, **6**, 836.

7.　(a) W. E. Cabrera, I. Schrooten, M. E. De Broe, P. C. D' Haese, *J. Bone Miner. Res.*, 1999, **14**, 661; (b) K. Liepe, J. Kotzerke, *Nucl. Med. Comm.,* 2007, **28**, 623; (c) Y. Henrotin, A. Labasse, S. X. Zheng, P. Galais, Y. Tsouderos, J. M. Crieland; J. Y. Reginster, *J. Bone Miner. Res.,* 2001, **16**, 299.

8.　(a) W. Zhou, Y. Y. Zhu, C. Q. Jiao, Z. G. Sun, S. P. Shi, L. L. Dai, T. Sun, W. Z. Li, M. X. Ma and H. Luo, *CrystEngComm.*, 2014, **16**, 1174; (b) S. P. Shi, Y. Y. Zhu, Z. G. Sun, W. Zhou, L. L. Dai, M. X. Ma, W. Z. Li, H. Luo, and T. Sun, *Cryst. Growth Des.*, 2014, **14**, 1580; (c) L. L. Dai, Y. Y. Zhu, C. Q. Jiao, Z. G. Sun, S. P. Shi, W. Zhou, W. Z. Li, T. Sun, H. Luo and M. X. Ma, *CrystEngComm.*, 2014, **16**, 5050.

9.　S. Bauer, T. Bein, N. Stock, *J. Solid State Chem.*, 2006, **179**, 145.

10.　K. D. Demadis, M. Papadaki, R. G. Raptis, H. Zhao, *J. of Solid State Chem.*, 2008, **181**, 679.

11. (a) K. D. Demadis, E. Armakola, K. E. Papathanasiou, G. Mezei, and A. M. Kirillov, *Cryst. Growth Des.*, 2014, **14**, 5234; (b) S. Bauer, N. Stock, *J. Solid State Chem.*, 2007, **180**, 3111.

12. J. L. Song, A. V. Prosvirin, H. H. Zhao, J. G. Mao, *Eur. J. Inorg. Chem.*, 2004, 3706.

13. W. Chu, Y. Y. Zhu, Z. G. Sun, C. Q. Jiao, J. Li, S. H. Sun, H. Tian and M. J. Zheng, *RSC Adv.*, 2013, **3**, 623.

14. J. L. Song, J. G. Mao, *J. Mol. Struc.*, 2005, **740**, 181.

15. (a) A. Cabeza, X. Ouyang, C. V. K. Sharma, M. A. G. Aranda, S. Bruque and A. Clearfield, *Inorg. Chem.*, 2002, **41**, 2325; (b) Z. M. Sun, J. G. Mao, B. P. Yang and S. M. Ying, *Solid State Sci.*, 2004, **6**, 295.

16. (a) A. Thirumurugan and S. Natarajan, *Dalton Trans.*, 2004, 2923; (b) Y. Q. Tang, W. H. He, Y. L. Lu, J. Fielden, X. Xiang and D. P. Yan, *J. Phys. Chem. C*, 2014, **118**, 25365; (c) D. Niu, J. Yang, J. Guo, W. Q. Kan, S. Y. Song, P. Du and J. F. Ma, *Cryst. Growth Des.*, 2012, **12**, 2397; (d) D. P. Yan, Y. Q. Tang, H. Y. Lin and D. Wang, *Sci. Rep.*, 2014, **4**, 4337; (e) J. Rocha, L. D. Carlos, F. A. A. Paz and D. Ananias, *Chem. Soc. Rev.*, 2011, **40**, 926; (f) F. Y. Li, J. P. Li, D. Wu, Y. Q. Lan and Z. M. Sun, *Mater. Horiz.*, 2015, **2**, 245.

17. (a) J. Li, C. C. Ji, L. F. Huang, Y. Z. Li and H. G. Zheng, *Inorg. Chim. Acta*, 2011, **371**, 27; (b) X. Q. Liu, Y. Y. Liu, Y. J. Hao, X. J. Yang and B. Wu, *Inorg. Chem. Commun.*, 2010, **13**, 511; (c) J. H. Wang, G. M. Tang, T. X. Qin, S. C. Yan, Y. T. Wang, Y. Z. Cui, *J. of Solid State Chem.*, 2014, **219**, 55.

18. (a) M. D. Allendorf, C. A. Bauer, R. K. Bhakta and R. J. T. Hook, *Chem. Soc. Rev.*, 2009, **38**, 1330; (b) B. B. Guo, L. Li, Y. Wang, Y. Y Zhu and G. Li, *Dalton Trans.*, 2013, **42**, 14268.

19. W. Zhou, J. Zhang, Z. G. Sun, Y. Y. Zhu, C. Q. Jiao, S. P. Shi, L. L. Dai, T. Sun, W. Z. Li, M. X. Ma, H. Luo, *Inorg. Chem. Comm.*, 2014, **47**, 37.

20. (a) D. Y. Ma, W. X. Wang, Y. W. Li, J. Li, C. Daiguebonne, G. Calvez, and O. Guillou, *CrystEngComm,* 2010, **12**, 4372; (b) Y. F. Xiao, T. T. Wang and H. P. Zeng, *J. Solid State Chem.*, 2015, **221**, 37.

21. (a) R. B. Fu, S. M. Hu and X. T. Wu, *CrystEngComm.*, 2011, **13**, 2331; (b) K. L. Wong, G. L. Law, Y. Y. Yang and W. T. Wong, *Adv. Mater.,* 2006, **18**, 1051; (c) D. P. Yan, G. O. Lloyd, A. Delori, W. Jones, X. Duan, *ChemPlusChem*, 2012, 77, 1112.

22. (a) B. L. Chen, Y. Yang, F. Zapata, G. N. Lin, G. D. Qian and E. B. Lobkovsky, *Adv. Mater.,* 2007, **19**, 1694; (b) Z. Y.Guo, H. Xu, S. Q. Su, J. F. Cai, S. Dang, S. C. Xiang, G. D. Qian, H. J.

Zhang, M. O'Keeffeand and B. L. Chen, *Chem. Commun.,* 2011*,* **47**, 5552; (c) H. Xu, F. Liu, Y. J. Cui, B. L. Chen and G. D. Qian, *Chem. Commun.,* 2011, **47**, 3153; (d) Y. W. Li, J. R. Li, L. F. Wang, B. Y. Zhou, Q. Chen and X. H. Bu, *J. Mater. Chem. A*, 2013, **1**,495.

23. (a) Y. A. Li, S. K. Ren, Q. K. Liu, J. P. Ma, X. Y. Chen. H. M. Zhu, *Inorg. Chem.,* 2012, **51**, 9629; (b) Y. Q. Chen, G. R. Li, Z. Chang, Y. K. Qu, Y. H. Zhang and X. H. Bu, *Chem. Sci.*, 2013, **4**, 3678; (c) D. P. Yan, R. Gao, M. Wei, S. D. Li, J. Lu, D. G. Evans and X. Duan, *J. Mater. Chem. C*, **1**, 997.

24. S. Bauer, T. Bein and N. Stock, *Inorg. Chem.*, 2005, **44**, 5882.

25. G. M. Sheldrick, *Acta Crystallogr., Sect. A: Found. Crystallogr.*, 2008, **64**, 112.